SIMULATION OF THE SUPPORT-ENCLOSING ROCK MASS INTERACTION FOR DEEP MINING

V. Kyrychenko[1], S. Stovpnyk[2*]

[1]LLC "West Donbas Research and Production Center "Geomechanics", Pavlohrad, Ukraine
[2]National Technical University of Ukraine "Igor Sikorsky Kyiv Polytechnic Institute", Kyiv, Ukraine
*Corresponding author: e-mail stovpnik@geobud.kpi.ua, tel. +3804420480085, fax: +380442048228

ABSTRACT

Purpose. To develop analytical model for a support-enclosing rock interaction to determine parameters for operational stability of deep mine workings while decreasing metal consumption and increasing efficient use of resources.

Methods. Involving various strength degradation functions and variations of physical and mechanical properties of rocks, mathematical modeling is used to consider the ranges of force action of a support on the enclosing rock mass of deep mine workings.

Findings. Analytical dependence of a support effect on the rock border displacement as well as on the changes in cross section of the mine working has been obtained. Effective interval of the support force resistance to block limit zones of the rock mass deformations has been substantiated. Innovative approach relying on the priority of the support working capacity as well as its forming characteristics has been proposed. The results of the studies help regulate the use of available supports, and the development of new designs meeting the increased geomechanical requirements of deep mining.

Originality. It has been determined for the first time that $150 - 250$ kN/m^2 interval of a support resistance is the most efficient and achievable; while mining deepening (more than 1000 m), a support resistance achieves $350 - 400$ kN/m^2. Higher values are not practical.

Practical implications. The results of the studies help regulate the use of available supports, and the development of new designs meeting the increased geomechanical requirements of deep mining and to determine the required parameters of both force and deformational characteristics of supports making.

Keywords: mathematical modeling, physical and mechanical properties, support of mine working, enclosing rock mass, resistance of a support

1. INTRODUCTION

The development of "support – rock mass" interaction system is driven by a requirement for the reliable forecasting of stability of mine workings as well as for the allowable limits determining reaction pressure of a support on a value of rock displacements (Baranowski & Lugovoi, 2008; Elmo & Stead, 2010; Gaidachuk, Koshel', & Lugovoi, 2011).

Convergence of calculation data with experiments concerning the use of the supports having related working characteristics are the criterion of the model accordance with actual conditions (Carranza-Torres & Fairhurst, 2000; Kononenko, Petlovanyi, & Zubko, 2015). Consideration of real values of the support efficiency along with its stable resistance is the essential objective. It is expedient to solve the problem in the context of al-lowable limits of the support actual effect on the value of finite displacements and estimation of the results – in the context of initial assumptions effect on the actual nature of the process physics.

The most important moment is the mechanical strength of the rock mass within a limit zone which consideration makes it possible to single out the three groups of calculation schemes:

1) according to its properties, a medium of the limit zone is identified with ideally flowing one; in this context, rock properties are taken up as similar for any point of the limit zone;

2) according to its properties, a medium of the limit zone corresponds to flowing medium with adhesion; its properties are also similar for any limit zone; however, its adhesion value differs from zero;

3) adhesion within the limit zone is taken up as a variable, and its value for each point of the limit zone is determined by means of strength degradation function.

While selecting a type of deformational strength degradation, the assumed function is quasi-similar to out-of-limit deformation diagram leg in the context of complicated stress state ($\sigma_3 \neq 0$) and, being undefinable, it should satisfy the two basic requirements: be continuous, and correspond to border conditions within external boundary of the limit zone as well as within its internal boundary (Stovpnyk, Borodai, & Kravets, 2011; Stovpnyk, Han, Zahoruiko, & Shaidetska, 2017).

As additional conditions, it is assumed that in the context of low values of wall pressure within boundary share of the limit zone ($\sigma_r \rightarrow P$), disintegration of material and its behaviour are followed by volumetric deformation, and deformational strength degradation with brittle failure prevailing (Stovpnyk & Osypov, 2017).

The effect of the increase in the support resistance ($p = \sigma_3$) is implemented as a result of degree dilatancy degree reduction (ε_v) as well as mobilization of the residual strength of disintegrated part of rock mass neighbouring the border.

It is possible to subdivide the available geomechanical solutions as follows:

– at the site of deep single mine working located beyond the area of mining influence as well as within a zone of front abutment pressure (up to the longwall "window"), a mode of interacting deformation is implemented in the context of rather heavy dependence of displacement value on the support working resistance; final balance the "support – neighbouring part of the rock mass" is achieved when the support resistance value is proper;

– effect of mining operations disturbs external limit balance on the line of limit disintegration zone and undisturbed rock mass being under the limit state one; due to the system balance disturbance, radius of the limit zone increases together with displacements within the mine working border as well as their velocity;

– generally, a new state of limit balance within a zone of front abutment pressure of a longwall is not achieved as the process is temporal; thus, the required support strengthening just decreases displacements down to a value providing necessary conditions of the mine working operations until the moment of its abandonment after the longwall advance; rate of advance determines a degree of cross-section reduction during the influence of geodynamic zone.

It should be noted that the idea of limit balance does not imply absolute attenuation of displacement; thus, it can be characterized when displacement velocity drops from its initial values being several dozens of millimeters a day down to less than $0.2 - 0.5$ mm/day. Within a zone of front abutment pressure, the displacements may near the values if only the zone obtains its final extension, i.e. after the longwall stoppage.

Consideration of the approaches makes it possible to apply the following (Hudson & Harrison, 2000; Jing, 2003; He, Xie, Peng, & Jiang, 2005; Jaeger, Cook, & Zimmerman, 2009; Brady & Brown, 2013; Wittke, 2014):

– in the context of extended mine working it is expedient to consider weightless plane as an initial state. The plane is weakened by a cut which form corresponds to a cross-section of a mine working with remote stresses being equal to stresses within undisturbed rock mass in the central part of a future mine working (A.I. Dinnik, A.V. Morgaevski, G.I. Savin);

– in the context of deep mine workings initial stress state may be assumed as hydrostatic (K.V. Ruppeneit, Yu.M. Liberman, M.A. Dolgikh, P. Mindlin and others);

– within the areas of the highest stress concentration in the neighbourhood of a mine working border, active stresses may exceed rock strength limit; in this context, brittle failure is a predominant type of rock deformation being typical for coal deposits (G.N. Kuznetsov, A.D. Panov, K.V. Ruppeneit, Yu.M. Liberman and others);

– in the function of limit balance of rock which deformations are followed by their brittle failure, it is possible to be limited to the consideration of rectilinear inclined compound curve since in the context of initial hydrostatic stress state, normal stresses acting within the mine working boundary are always situated behind the circle of uniaxial compression; upon that, consideration of differences in locations of compound curves for disturbed rocks and undisturbed ones is mandatory (A. Labass, K.V. Ruppeneit, Yu.M. Liberman and others);

– in the context of calculations concerning a mine working which form of cross section differs from circular one to simplify data, the substitution for equivalent circular cannot introduce significant error into final results; maximum difference of the latter is not more than 10% (K.V. Ruppeneit, M.A. Dolgikh);

– currently, it is possible to consider the effect of anisotropy of real rocks on the displacement and distribution of stresses around a mine working (S.G. Lekhnitski, A.N. Zorin, M.I. Rozovski); however, if analytical studies are meant, the idea to consider anisotropy of real rock masses in terms of empirical coefficients is the most reasonable; moreover, since analytical studies of such a type should be performed together with a field experiment, its numerical value may be obtained according to the observation results.

Thus, there is abundance of experimental data for substantiated selection of a type of functions of deformational strength degradation within different points of limit zone and to reduce the number of functions, taken for the analysis in terms of the specified calculation technique.

2. CALCULATION MODEL OF A BORDER DISPLACEMENT AND DETERMINATION OF PRESSURE ACTING ON THE SUPPORT OF A MINE WORKING

Since volumetric deformation (i.e. dilatation in the process of pseudoplastic deformations) is the basic factor determining final value of displacements in terms of rock border of a mine working, the use of a known condition of plastic potential is necessary:

$$\varepsilon_\theta = \lambda \,;\; \varepsilon_r = -\lambda \left(1 + \frac{df_r}{df_r} \right), \tag{1}$$

where:

λ – arbitrary parameter;

f_r – plasticity function describing rock behaviour $f_{(\sigma_r)} = \sigma_\theta - \sigma_r$.

Since, effect of a support resistance on the value of final displacements of a mine working border of cross section is in large part determined by a type of a function of distribution (strength degradation), the development of the mathematical model should involve the three relevant functions: exponential, rational, and hyperbolical.

Consider rock mass assuming it as homogenous isotropic medium where both elastic and nonelastic deformations arise after the development of a mine working (Fig. 1).
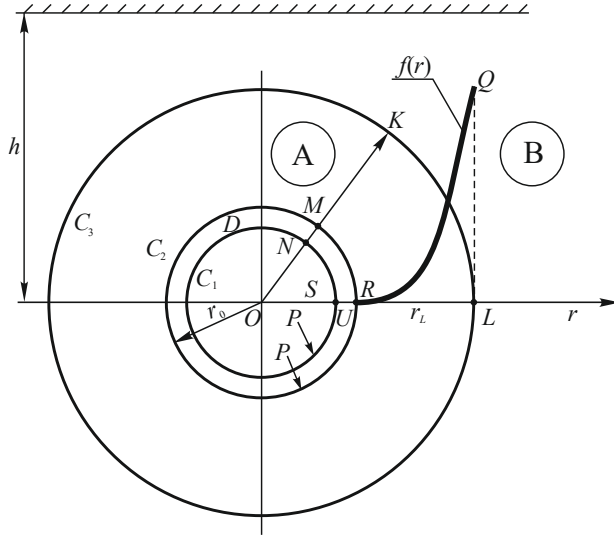

Figure 1. Design model for elastic and nonelastic defor-mations calculation

Mainly, nonelastic deformations are represented in the form of pseudoplastic brittle deformations. Round mine working is located at rather large distance h from the surface and stress state is of hydrostatic type (Poisson's ratio is $v = 0.5$), i.e. axisymmetric plane problem is under consideration.

Introduce following symbols:
C_1 – a circle with r_0 radius $U(OM - ON = OR - OS = U)$;
C_2 – a circle with r_0 radius ($r_0 = OM = OR$);
C_3 – a circle with r_L radius ($r_L = OK = OR$).

Mark a zone of pseudoplastic deformations A within the specified plane A (A is a zone between C_2 and C_3 circles); a zone of elastic deformations B (B is a zone located beyond the C_3 circle); zone D (D is a zone between C_1 and C_2 circles) characterizing the cross section decrease by the time when final balance of "support – rock mass" approaches.

Support displacements are determined with the help of the value:

$$U = OM - ON \text{ (or } U = OR - OS), \tag{2}$$

where:
r_0 – the radius of a circle of a mine working to which uniformly distributed pressure P is applied.

Find a change in relative area of the failure zone, i.e. area of zone D classified as a part of a circle area with r_0 radius. It is obvious that since area of S circle with R radius is equal to πR^2, then area of zone D is equal to $\pi (r_0^2 - (r_0 - U)^2)$, i.e.:

$$\frac{\Delta S}{S} = \frac{\pi \left(r_0^2 - (r_0 - U)^2 \right)}{\pi r_0^2} = \frac{U(2r_0 - U)}{r_0^2}. \tag{3}$$

2.1. Determination of stresses

Plasticity equation within A zone is:

$$\sigma_\theta - \sigma_r = \alpha_2 \sigma_r + R_{st} f(r), \tag{4}$$

where:
σ_r – radial stresses;
σ_θ – tangential stresses;
$\alpha_2 = 2\sin \varphi_1 / 1 - \sin \varphi$, R_{st} – maximum rock strength;
$f(r)$ – function approximation dependence σ_{st} / R_{st}.
Balance equation takes place for σ_r, σ_θ values:

$$\frac{d\sigma_r}{dr} + \frac{\sigma_r - \sigma_\theta}{r} = 0. \tag{5}$$

Specify radial deformations and tangential deformations by means of ε_r and ε_θ respectively. Then, compatibility condition of deformations within A zone is:

$$\frac{d\varepsilon_r}{dr} + \frac{\varepsilon_\theta - \varepsilon_r}{r} = 0. \tag{6}$$

It should be pointed out that at infinity (if $r \to +\infty$), normal stress components are equal to each other; $\tau_\theta = 0$:

$$\sigma_r = \sigma_\theta = \gamma h. \tag{7}$$

Interpretation of formula (4) is that strength properties of material (rock) may be described with the help of rectilinear compound curve of stress circles: $\tau = \sigma \, \text{tg} \, \varphi_1 + K$, where φ_1 is friction angle.

Write down formula (4) in another way:

$$\sigma_\theta - \sigma_r = \psi(\sigma_r); \ \psi(\sigma_r) = \alpha_2 \sigma_r + R_{st} f(r). \tag{8}$$

Then, using properties of zone A and a condition of plastic potential, following formulas for ε_r and ε_θ deformation can be written down in the form of:

$$\varepsilon_0 = \lambda; \ \varepsilon_r = -\lambda \left(1 + \frac{d\psi}{dr} \right). \tag{9}$$

In view of ratio two from (8) for ε_r from (9) we get:

$$\varepsilon_r = -\lambda \left(1 + R_{st} \frac{df(r)}{dr} + \alpha_2 \frac{d\sigma_r(r)}{dr} \right). \tag{10}$$

While integrating equations (5) and (6) in which specifications (8) are introduced, we will use boundary conditions:

$$\sigma_r = \sigma_\theta = \gamma h, \text{ if } r = \infty; \tag{11}$$

$$\sigma_r = P, \text{ if } r = r_0, \tag{12}$$

where:
P – the support resistance with $p = const$ characteristic.
In Figure 1, r_L means a value characterizing radius of circle C_3 separating elastic zone B and failure zone A.
In view of continuity it is necessary to assume that:

$$\begin{cases} \sigma_r^{(A)} = \sigma_r^{(B)}; \\ \varepsilon_r^{(A)} = \varepsilon_r^{(B)}; & \text{if } r = r \\ \sigma_\theta^{(A)} - \sigma_\theta^{(B)} = \psi(\sigma_r). \end{cases} \tag{13}$$

For a function $f(r)$ shown in Figure 1 by means of separated line, following equalities hold true:

$$f(r_0) = 0 \; ; \; f(r_L) = 1 \; . \qquad (14)$$

In addition, we consider implying:

$$\sigma_{r_L} = (1 - \sin\varphi_1)\left(\gamma h - \frac{R_{st}}{2}\right) . \qquad (15)$$

Insert expression (7) in formula (4):

$$\frac{d\sigma_r}{dr} = \alpha_2 \frac{\sigma_r}{r} + R_{st} \frac{f(r)}{r} \; . \qquad (16)$$

Equation (16) is a differential first-order equation. Hence, we will seek its solution with the help of a method of variation of arbitrary constant. First consider the homogeneous equation $\dfrac{d\sigma_r}{dr} = \alpha_2 \dfrac{\sigma_r}{r}$, or, representing it in another way $\dfrac{d\sigma_r}{\sigma_r} = \alpha_2 \dfrac{dr}{r}$, we obtain:

$$\int \frac{d\sigma_r}{\sigma_r} = \alpha_2 \int \frac{dr}{r} \rightarrow \sigma_r = C(\sigma_r) r^{\alpha_2} \; . \qquad (17)$$

The above formula is required to seek a solution for nonhomogeneous equation (16). While replacing σ_r from equation (17) to equation (16) we obtain:

$$\frac{dC(\sigma_r)}{d\sigma_r} = R_{st} \frac{f(r)}{r^{\alpha_1}} ; \; \alpha_1 = \frac{1 + \sin\varphi_1}{1 - \sin\varphi_1} \; . \qquad (18)$$

Equation (18) gives ratio for $C(\sigma_r)$:

$$C(\sigma_r) = R_{st} \int r^{-\alpha_1} f(r)dr + C \; , \qquad (19)$$

where:
C – arbitrary constant.

Basing upon (17) and (19) find general solution for equation (16):

$$\sigma_r = r^{\alpha_2}\left(R_{st}\int_{r_0}^{r} r^{-\alpha_1} f(r)dr + C\right) . \qquad (20)$$

Using boundary condition (12), we obtain final formula from (20):

$$\sigma_r = r^{\alpha_2}\left(R_{st}\int_{r_0}^{r} r^{-\alpha_1} f(r)dr + \frac{P}{r_0^{\alpha_2}}\right) . \qquad (21)$$

If availability of integral in formula (21) is taken into consideration, then function $\sigma_r(r)$ is a function of upper limit of an integral as well.

2.2. Determination of deformations

Inserting expressions (9) and (10) in differential equation (6) we get:

$$\frac{d\lambda}{dr} + \frac{\lambda}{r}\left(\alpha_3 + \frac{R_{st}^{\;r}}{\alpha_2\sigma_r + R_{st}f(r)} \cdot \frac{df(r)}{dr}\right) = 0 \; , \qquad (22)$$

where:

$$\alpha_3 = \frac{2}{1 - \sin\varphi} \; .$$

It is not difficult to demonstrate by means of direct differentiation that solution of the equation (22) is:

$$\lambda(r) = \frac{C^*}{r^2(\alpha_2\sigma_r + R_{st}f(r))} \; , \qquad (23)$$

where:
C^* – arbitrary constant.

Using $\varepsilon_\theta = \dfrac{U}{r}$ and $\varepsilon_r = \dfrac{dU}{dr}$ formulas, where $U(r)$ – movement, and formula (23), determine:

$$U(r) = \frac{C^*}{r(\alpha_2\sigma_r + R_{st}f(r))} \; . \qquad (24)$$

Apply boundary condition taking place if $r = r_L$ to determine a constant C^*.

Displacements within zone B are identified with the help of the expression:

$$U^{(B)} = \frac{1 + v}{E} \cdot \frac{M}{r} ; \; M = \frac{r_L^2}{\alpha_2}(\alpha_2\gamma h + R_{st}) . \qquad (25)$$

Hence, the C^* constant in (24) formula can be found from the equality condition of radial movements (24) and (25).

Formulate the results of the transformations under the condition that zone A (failure zone) arises:

$$U = \frac{2(1 + v)r_L^2(\alpha_2\gamma h + R_{st})^2}{Er_0\alpha_2\alpha_3^2 P} \qquad (26)$$

where:
v – Poisson's ratio;
E – Young's modulus.

Formulate the problem using the abovementioned approach. Assume that function $f(r)$ and parameters v, E, R_{st}, P, φ_1, r_0 have been set. Then, the problem solution involves two stages.

Stage one: in accordance with formulas (21) and (15) we have the equality:

$$r_L^{\alpha_2}\left(R_{st}\int_{r_0}^{r_L} r^{-\alpha_1} f(r)dr + \frac{P}{r_0^{\alpha_2}}\right) = $$
$$= (1 - \sin\varphi_1)\left(\gamma h - \frac{R_{st}}{2}\right), \qquad (27)$$

with the help of which, r_L value characterizing zones A and B. Since, left side contains integral then it is possible to determine r_L using numerical procedure.

Stage two: after determination of r_L all values of the parameters are inserted in formula (26); thus, the movement is being determined:

$$U = \frac{2(1 + v)r_L^2(\alpha_2\gamma h + R_{st})^2}{Er_0\alpha_2\alpha_3^2 P} \; . \qquad (28)$$

Stage three: while using formula (3), we have a graph of $\dfrac{\Delta s}{s}$ function depending upon pressure:

$$\frac{\Delta s}{s} = \frac{U(2r_0 - U)}{r_0^2} \; , \qquad (29)$$

where:

    U – a function of P.

    Besides, such a numerical approach makes it possible to determine qualitative dependences $U(r)$, $U(r_L)$ etc.

3. RESULTS OF THE NUMERICAL MODELING

    To perform a more comprehensive mechanical and mathematical modeling, consider following classes of function $f(r)$ relative to $(r - r_0)$ value.

3.1. Class one of $f(r)$ functions

    Define $f(r)$ function in exponential form:

$$f(r) = \beta_0 (r - r_0)^n e^{r/r_0} , \tag{30}$$

where:

    β_0 – a constant being determined with the help of the condition $f(r_L) = 1$, $\beta_0 = \dfrac{1}{(r_L - r_0)^n} e^{-r_L/r_0}$.

    Thus, formula (29) is:

$$f(r) = \frac{e^{-r_L/r_0}}{(r_L - r_0)^n} e^{r/r_0} (r - r_0)^n , \tag{31}$$

where:

    n – a whole number.

    It follows from formulas (27) and (31) that:

$$g_1(r_L) = g_2(r_L), \tag{32}$$

where:

$$g_1(r_L) = \int_{r_0}^{r_L} r^{-\alpha_1} (r - r_0)^n e^{r/r_0} dr ; \tag{33}$$

$$g_2(r_L) = \frac{(r_L - r_0)^n}{R_{st}} \left((1 - \sin\varphi_1) \times \right.$$
$$\left. \times \left(\gamma h - \frac{R_{st}}{2} \right) r_L^{-\alpha_2} - \frac{P}{r_0^{\alpha_2}} \right) e^{r/r_0} ; \tag{34}$$

    Equation (32) is the equation to identify r_L. It is convenient to solve it by means of graphoanalytical method that is a method of $g_1(r) = g_2(r)$ functions construction.

    After determination of r_L, use formula (28) to define U. Numerical experiment is demonstrated for the following example:

    $h = 1000$ m; $\gamma = 2.5$ t/m³;

    $E = 1.5 \cdot 10^6$ t/m²; $\nu = 0.3$;

    $R_{st} = 4000$ t/m²; $r_0 = 2.5$ m;

    $n = 2, 3, 4$; $\varphi_1 = 20°, 25°, 30°$.

    Table 1 shows results of the calculations.

Table 1. Results of the calculations for class one of f(r) functions

Parameter	P, t/m²	$n = 2$ angle φ_1			$n = 3$ angle φ_2			$n = 4$ angle φ_1		
		20°	25°	30°	20°	25°	30°	20°	25°	30°
r_L, m	10	3.23	3.09	2.97	3.57	3.35	3.17	4.01	3.67	3.40
	15	3.20	3.07	2.96	3.54	3.33	3.14	3.95	3.63	3.35
	25	3.17	3.04	2.93	3.48	3.27	3.09	3.84	3.53	3.27
U, m	10	3.27	2.22	1.55	4.01	2.61	1.76	5.06	3.12	2.03
	15	2.16	1.46	1.02	2.63	1.71	1.16	3.27	2.03	1.31
	25	1.27	0.86	0.60	1.52	0.99	0.67	1.85	1.15	0.75
$\dfrac{\Delta s}{s}$, %	10	90	98	85	63	99	91	—	93	96
	15	98	82	64	99	90	71	90	96	77
	25	75	57	42	84	63	46	36	70	51

3.2. Class two of $f(r)$ functions

    Assume that $f(r)$ function is of rational type as a ratio of polynomials:

$$f(r) = \frac{\beta_0 (r - r_0)^n}{r_0^2 + (r - r_0)^2} . \tag{35}$$

    In accordance with $f(r_L) = 1$, function (35) is:

$$f(r) = \frac{r_0^2 + (r_L - r_0)^2}{(r_L - r_0)^n} \cdot \frac{(r - r_0)^n}{r_0^2 + (r - r_0)^2} . \tag{36}$$

    With the help of formula (36) rewrite equality (27) as follows:

$$G_1(r_L) = G_2(r_L), \tag{37}$$

where:

$$G_1(r_L) = \int_{r_0}^{r_L} \frac{r^{-\alpha_2} (r - r_0)^n}{r_0^2 + (r - r_0)^2} dr ;$$

$$G_2(r_L) = \frac{(r_L - r_0)^n}{R_{st} \left(r_0^2 + (r_L - r_0)^2 \right)} \times$$
$$\times \left(r_L^{-\alpha_2} (1 - \sin\varphi_1) \left(\gamma h - \frac{R_{st}}{2} \right) - \frac{P}{r_0^{\alpha_2}} \right) . \tag{38}$$

    Like in the previous case, equation (37) with symbols (38) is solved by means of graphoanalytical method. Table 2 explains results of the calculations.

3.3. Class three of $f(r)$ functions

    Define $f(r)$ in the class of hyperbolic functions:

$$f(r) = \frac{\beta_0 (r - r_0)^n}{\left(r_L^{\max} - r \right)^k} , \quad n = 2,3...; k = 1,2... \tag{39}$$

    It is possible to determine β_0 while applying $f(r)$ value within r_L point: $f(r_L) = 1$.

Table 2. Results of the calculations for class two of f(r) functions

Parameter	P, t/m^2	$n=2$ angle φ_1			$n=3$ angle φ_2			$n=4$ angle φ_1		
		20°	25°	30°	20°	25°	30°	20°	25°	30°
r_L, m	10	3.15	3.05	2.95	3.41	3.04	3.12	3.71	3.50	3.31
	15	3.13	3.03	2.94	3.39	3.03	3.11	3.68	3.47	3.28
	25	3.10	3.01	2.91	3.35	3.00	3.06	3.61	3.41	3.22
U, m	10	3.10	2.10	1.53	3.50	2.10	1.71	4.31	2.84	1.93
	15	2.06	1.40	1.03	2.41	1.42	1.13	2.83	1.88	1.26
	25	1.20	0.80	0.59	1.41	0.84	0.66	1.64	1.08	0.73
$\frac{\Delta s}{s}$, %	10	—	97	84	—	97	90	—	98	94
	15	96	80	65	99	81	69	—	93	75
	25	72	53	41	80	55	45	88	67	50

Then the formula is a consequence of (39):

$$f(r) = \frac{\left(r_L^{\max} - r_L\right)^k}{\left(r_L - r_0\right)^n} \cdot \frac{\left(r - r_0\right)^n}{\left(r_L^{\max} - r_0\right)^k}. \tag{40}$$

$r_L^{\max}$ parameter may be selected additionally (e.g. $2r_L$, $3r_L...r_L$).

Value r_L is being determined with the help of the equation:

$$Q_1(r_L) = Q_2(r_L); \tag{41}$$

$$Q_1(r_L) = \int_{r_0}^{r_L} r^{-\alpha_2} \frac{\left(r - r_0\right)^n}{\left(r_L^{\max} - r_0\right)^k} dr; \tag{42}$$

$$Q_2(r_L) = \frac{\left(r_L - r_0\right)^n}{R_{st}\left(r_L^{\max} - r_L\right)^k} \times$$
$$\times \left(r_L^{-\alpha_2}\left(1 - \sin\varphi_1\right)\left(\gamma h - \frac{R_{st}}{2}\right) - \frac{P}{r_0^{\alpha_2}} \right). \tag{43}$$

Numerical experiment for (41) and (42) has been performed when $r_L^{\max} = 2r_0$, $k = 1$.

Table 3 demonstrates results concerning calculations of parameters r_L, U, and $\Delta s/s$.

Analysis of Tables 1, 2, and 3 obtained with the help of numerical experiment shows that more detailed studies are required when $\varphi_1 = 30°$ as well as in the context of the increase in the range of pressure values up to 55 t/m^2. Table 4 shows calculation results for all distribution functions $f(r)$ under study (cases 1, 2, and 3).

Table 3. Results of the calculations for class three of f(r) functions

Parameter	P, t/m^2	$n=2$ angle φ_1			$n=3$ angle φ_2			$n=4$ angle φ_1		
		20°	25°	30°	20°	25°	30°	20°	25°	30°
r_L, m	10	3.17	3.06	2.96	3.46	3.29	3.14	3.81	3.55	3.34
	15	3.15	3.04	2.94	3.43	3.27	3.12	5.00	3.52	3.31
	25	3.12	3.01	2.92	3.38	3.22	3.07	5.00	3.44	3.24
U, m	10	3.10	2.17	1.54	3.70	2.51	1.73	4.56	2.93	1.96
	15	2.08	1.43	1.07	2.40	1.65	1.14	5.23	1.91	1.28
	25	1.22	0.84	0.59	1.41	0.96	0.66	3.14	1.10	0.73
$\frac{\Delta s}{s}$, %	10	—	98	85	—	99	90	—	—	95
	15	97	81	67	99	88	70	—	94	76
	25	73	55	41	80	62	45	—	68	49

Figure 2 demonstrates generally the dependence of U, U/r_0, and $\Delta s/s$ parameters of the value of assumed resistance of support P (if $p = const$ characteristic is constant).

Relying upon the allowable values of rock displacements corresponding to a value of pliability of supports as well as to residual (required) area of the mine working cross section, such interval of the support resistance as $150 - 250$ kN/m^2 (being $60 - 120$ kN/m^2 in the context of standard arched supports) is technically the most efficient and achievable one. Depending upon the mining deepening ($H > 1000$ m), the efficient interval P may expand up to $350 - 400$ kN/m^2; further expansion is unreasonable.

Analysis the results of the model concerning the interaction between force parameter of a support and displacements of neighbouring rock mass involves the ne-

cessity to mention sufficient convergence of the obtained theoretical results and the results of full-scale experiments providing an opportunity to expect the development of a new reference document specifying the problems of practical implementation of both available supports and the development of new ones corresponding to complicated geomechanical conditions.

Mining deepening predetermined the necessity in the innovative scientific approach developed by us. The approach is based upon the significance of a performance parameter of a support (Q) as well as characteristics forming it – working resistance (P_r) and structural pliability (Δ) owing to common physical content of the process as an activity providing the formation of "support – rock mass" system: $Q = P_r \times \Delta$.

Table 4. Results of the calculations for all distribution of f(r) functions

| Parameter	P, t/m²	case 1			case 2			case 3		
		$n = 2$	$n = 3$	$n = 4$	$n = 2$	$n = 3$	$n = 4$	$n = 2$	$n = 3$	$n = 4$
		angle $\varphi_1 = 30°$			angle $\varphi_1 = 30°$			angle $\varphi_1 = 30°$		
		20°	25°	30°	20°	25°	30°	20°	25°	30°
r_L, m	5	2.99	3.20	3.45	2.97	3.15	3.35	3.01	3.23	3.50
	10	2.97	3.17	3.40	2.96	3.13	3.31	2.99	3.20	3.44
	15	2.96	3.14	3.35	2.94	3.28	2.10	2.97	3.17	3.39
	25	2.93	3.09	3.27	2.91	3.07	3.22	2.94	3.30	3.11
	40	2.70	2.80	2.81	2.88	3.01	3.14	2.90	3.04	3.20
	55	2.55	2.48	2.50	2.84	2.95	3.07	2.86	2.98	3.11
U, m	5	3.14	3.60	4.17	3.09	3.48	3.93	3.18	3.66	4.30
	10	1.55	1.76	2.03	1.53	1.72	1.93	1.57	1.79	2.08
	15	1.02	1.16	1.31	1.01	1.13	1.26	1.03	1.17	1.34
	25	0.60	0.67	0.75	0.59	0.66	0.73	0.61	0.68	0.77
	40	0.30	0.41	0.49	0.36	0.39	0.43	0.37	0.41	0.44
	55	0.19	0.20	0.21	0.26	0.27	0.30	0.26	0.28	0.38
$\dfrac{\Delta s}{s}$, %	5	99	92	—	94	84	67	92	78	47
	10	85	91	96	85	90	94	86	92	97
	15	64	71	77	64	70	75	65	72	78
	25	42	46	51	42	46	49	43	47	52
	40	22	35	30	27	29	31	27	30	32
	55	14	16	16	19	21	22	19	21	23
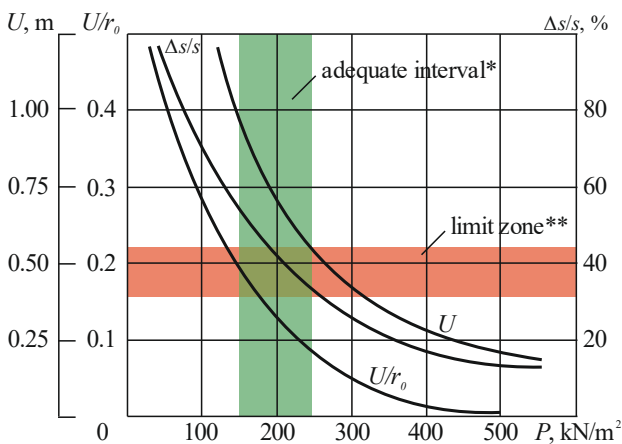
*Figure 2. Effect of support P resistance of the displacement of rock border U, U/r₀ and relative change in a cross section Δs/s of a mine working: *adequate interval of power resistance of the support; **limit zone of rock displacement blockage*

In this context, a parameter of limiting bearing capability of a support (P_s) is the determinant of the possibility to increase working support (P_r) as well as the efficiency of the design (Q).

4. CONCLUSIONS

1. Irrespective of approaches of mathematical modeling connected with the selection of distribution function $f(r)$, sufficient convergence of numerical results of changes in r_L and U values in the context of variability of a support resistance has been obtained; the fact is illustrative of the adequacy of actually covered process concerning the "support – rock mass" system interaction.

2. Dependence of changes in r_L and U values is the most suitable for both experimental and practical data if $n = 2$, $\varphi_1 = 30°$.

3. A zone of plastic deformation is characterized by the fact that its dimension ($r_L - r_0$) in all modeling cases despite the properties of material, remains to be within a meter or two being important physically and useful practically.

4. The stated approach as well as the statement of the modeling problem made it possible to obtain general solution in the context of different types of strength degradation function giving more accurate results to approach the practice.

5. The obtained results help formulate reasonably the initial requirements for both power and kinematic parameters of supports belonging to a new technical level. Support becomes operationally adequate when its resistance is within 150 – 250 kN/m². Depending upon the mining deepening ($H > 1000$ m), the efficient interval P may expand up to 350 – 400 kN/m²; further expansion is unreasonable.

6. Innovative approach based upon the use of a support performance parameter as well as forming characteristics (i.e. working resistance and structural pliability) has been proposed. The approach makes it possible to design new structures for supports in mine workings.

ACKNOWLEDGEMENTS

REFERENCES

Baranowski, Z., & Lugovoi, P.Z. (2008). Stress-Strain State Near Mine Workings in Anisotropic Rock Masses Under the Action of Discontinuous Waves. *International Applied Mechanics*, *44*(4), 406-412.
https://doi.org/10.1007/s10778-008-0052-z

Brady, B.H., & Brown, E.T. (2013). *Rock Mechanics: For Underground Mining*. New York: Springer Science & Business Media.
https://doi.org/10.1007/978-1-4020-2116-9_1

Carranza-Torres, C., & Fairhurst, C. (2000). Application of the Convergence-Confinement Method of Tunnel Design to Rock Masses That Satisfy the Hoek-Brown Failure Criterion. *Tunnelling and Underground Space Technology*, 15(2), 187-213.
https://doi.org/10.1016/s0886-7798(00)00046-8

Elmo, D., & Stead, D. (2010). An Integrated Numerical Modelling-Discrete Fracture Network Approach Applied to the Characterisation of Rock Mass Strength of Naturally Fractured Pillars. *Rock Mechanics and Rock Engineering*, 43(1), 3-19.
https://doi.org/10.1007/s00603-009-0027-3

Gaidachuk, V.V., Koshel', V.I., & Lugovoi, P.Z. (2011). Stress Distribution Around Mine Workings. *International Applied Mechanics*, 46(9), 981-986.
https://doi.org/10.1007/s10778-011-0388-7

He, M.C., Xie, H.P., Peng, S.P., & Jiang, Y.D. (2005). Study on Rock Mechanics in Deep Mining Engineering. *Chinese Journal of Rock Mechanics and Engineering*, 24(16), 2803-2813.

Hudson, J.A., & Harrison, J.P. (2000). *Engineering Rock Mechanics: An Introduction to the Principles*. New York: Elsevier.
https://doi.org/10.1115/1.1451165

Jaeger, J.C., Cook, N.G., & Zimmerman, R. (2009). *Fundamentals of Rock Mechanics*. Hoboken: John Wiley & Sons.
https://doi.org/10.1086/627658

Jing, L. (2003). A Review of Techniques, Advances and Out-Standing Issues in Numerical Modelling for Rock Mechanics and Rock Engineering. *International Journal of Rock Mechanics and Mining Sciences*, 40(3), 283-353.
https://doi.org/10.1016/s1365-1609(03)00013-3

Kononenko, M., Petlovanyi, M., & Zubko, S. (2015). Formation the Stress Fields in Backfill Massif Around the Chamber with Mining Depth Increase. *Mining of Mineral Deposits*, 9(2), 207-215.
https://doi.org/10.15407/mining09.02.207

Stovpnyk, S.N., Borodai, S.V., & Kravets, V.G. (2011). The Stressed-Deformed State of the Underground Tunnel Processing of Shallow Watering in Water-Saturated Sands. In *Proceedings of the Third Scientific and Technical Conference "Power engineering. Ecology. MAN"* (pp. 112-114). Kyiv: NTUU KPI.

Stovpnyk, S.M., Han, A.L., Zahoruiko, E.A., & Shaidetska, L.V. (2017). Research of Hydraulic Impact on the Technological Stability of Shallow Metrotunnel in Dredging Massives. *Science and Transport Progress. Bulletin of Dnipropetrovsk National University of Railway Transport*, 5(71), 141-148.

Stovpnyk, S.N., & Osypov, A.S. (2017). The Geomechanical Confirmation of Methods for Stabilization of Tectonic Mass Rocks for Period of Building the Tunnel of Biggest Dimensions. *Visnyk Natsionalnoho Tekhnichnoho Universytetu "KPI". Seria "Hirnyctvo"*, (34), 17-27.

Wittke, W. (2014). *Rock Mechanics Based on an Anisotropic Jointed Rock Model (AJRM)*. Berlin: John Wiley & Sohn.
https://doi.org/10.1002/9783433604281

МОДЕЛЮВАННЯ ВЗАЄМОДІЇ КРІПЛЕННЯ Й МАСИВУ, ЩО МІСТИТЬ ВИРОБКУ ГЛИБОКОГО ЗАКЛАДЕННЯ

В. Кириченко, С. Стовпник

Мета. Розробка аналітичної моделі взаємодії кріплення й масиву для визначення параметрів забезпечення експлуатаційної стійкості гірничих виробок на великих глибинах, зниження їх металоємності та підвищення ресурсозбереження.

Методика. Математичним моделюванням із залученням різних функцій знеміцнення та варіації фізико-механічних властивостей гірських порід розглянуті діапазони силових впливів кріплення на масив, що містить виробку глибокого закладення.

Результати. Встановлено аналітичну залежність впливу кріплення на зміщення породного контуру та зміну площі перерізу виробки. Обґрунтовано ефективний інтервал силового опору кріплення для блокування граничних зон деформацій масиву. Досліджено параметри працездатності кріплення та його утворюючих характеристик – робочого опору та конструктивної піддатливості як роботи, що забезпечує формування системи "кріплення – масив».

Наукова новизна. Запропоновано новий науковий підхід, заснований на пріоритетності параметра працездатності кріплення та його утворюючих характеристик. Вперше встановлено, що найбільш ефективним і реально досяжним є інтервал опору кріплення 150 – 250 кН/м², зі збільшенням глибини ведення гірничих робіт понад 1000 м опір кріплення сягає 350 – 400 кН/м², а більш – є недоцільним.

Практична значимість. Результати досліджень з достатньою для практичного застосування точністю можуть використовуватися для визначення необхідних параметрів силових і деформаційних характеристик кріплень, дозволяють регламентувати практику використання існуючих кріплень та розробку нових конструкцій, що відповідають підвищеним геомеханічним вимогам великих глибин розробки.

Ключові слова: математичне моделювання, фізико-механічні властивості, кріплення гірничих виробок, масив, опір кріплення

МОДЕЛИРОВАНИЕ ВЗАИМОДЕЙСТВИЯ КРЕПИ И ВМЕЩАЮЩЕГО МАССИВА ДЛЯ ВЫРАБОТКИ ГЛУБОКОГО ЗАЛОЖЕНИЯ

В. Кириченко, С. Стовпник

Цель. Разработка аналитической модели взаимодействия крепи и вмещающего массива для определения параметров обеспечения эксплуатационной устойчивости горных выработок на больших глубинах, снижения их металлоемкости и повышения ресурсосбережения.

Методика. Математическим моделированием с привлечением различных функций разупрочнения и вариации физико-механических свойств горных пород рассмотрены диапазоны силовых воздействий крепи на вмещающий массив выработок глубокого заложения.

Результаты. Получена аналитическая зависимость влияния крепи на смещение породного контура и изменения площади сечения выработки. Обоснован эффективный интервал силового отпора крепи для блокировки предельных зон деформаций массива. Исследованы параметры работоспособности крепи и образующих его характеристик – рабочего сопротивления и конструктивной податливости как работы, обеспечивающей формирование системы "крепь – массив".

Научная новизна. Предложен новый научный подход, основанный на приоритетности параметра работоспособности крепи и его образующих характеристик. Впервые установлено, что наиболее эффективным и реально достижимым является интервал отпора крепи $150 - 250$ кН/м^2, с увеличением глубины ведения горных работ более 1000 м отпор крепи может достигать $350 - 400$ кН/м^2, а более – является нецелесообразным.

Практическая значимость. Результаты исследований с достаточной для практического применения могут использоваться для определения необходимых параметров силовых и деформационных характеристик крепей, позволяют регламентировать практику использования существующих крепей и разработку новых конструкций, отвечающих повышенным геомеханическим требованием больших глубин разработки.

Ключевые слова: математическое моделирование, физико-механические свойства, крепь горных выработок, вмещающий массив, отпор крепи

ARTICLE INFO

ABOUT AUTHORS

Volodymyr Kyrychenko, Doctor of Technical Sciences, Director of the LLC "West Donbas Research and Production Center "Geomechanics", 9/1 Tereshkina St, 51400, Pavlohrad, Ukraine. E-mail: geomeh.krp@gmail.com

Stanislav Stovpnyk, Candidate of Technical Sciences, Head of the Geoengineering Department, National Technical University of Ukraine "Igor Sikorsky Kyiv Polytechnic Institute", 37 Peremohy Ave., 03056, Kyiv, Ukraine. E-mail: stovpnik@geobud.kpi.ua